

# Solvent Properties of Liquid and Supercritical 1,1,1,2-Tetrafluoroethane

Andrew P. Abbott\* and Christopher A. Eardley

Chemistry Department, Leicester University, Leicester, LE1 7RH, United Kingdom

Received: January 16, 1998; In Final Form: July 13, 1998

The polarizability parameter,  $\pi^*$  from the theory of Kamlet and Taft was measured for 1,1,1,2-tetrafluoroethane (HFC 134a) as a function of temperature and pressure, to cover the liquid and supercritical states. The polarizability changed with the reduced density of the fluid and three distinct density regions were observed. The relative permittivity was also measured over the range 30–130 °C and 40–300 bar and used to model the  $\pi^*$  data. The mean sphere approximation (MSA) model was applied to the data and found to produce an excellent fit to the data in both the liquid and supercritical states. The values of  $\pi^*$  are also shown to have good correlation to the solubility of water in these media.

## Introduction

Supercritical (sc) fluids are primarily of interest because of the marked change in solvation properties that can occur with relatively modest changes in temperature or pressure. They have primarily been used for extraction<sup>1,2</sup> and chromatography.<sup>3,4</sup> Most work has been carried out with carbon dioxide due to the mild critical temperature and pressure ( $T_c = 304.3$  K;  $P_c = 73.8$  bar), low cost, and lack of toxicity. Physicochemical properties such as density, relative permittivity, and viscosity can change by up to an order of magnitude close to the critical point and this has a significant effect on the solubility of species in the sc fluids.

The solvent properties of supercritical fluids have been determined by the solvatochromic shift method, primarily using the polarity/polarizability parameter,  $\pi^*$ , defined by Kamlet and Taft.<sup>5,6</sup> Sigman et al.<sup>7</sup> measured  $\pi^*$  for a number of solvatochromic indicator solutes in  $\text{scCO}_2$ . It was found that there was a relationship between the solvent density and  $\pi^*$ . The values for all of the fluids tested were less than those for cyclohexane, showing that  $\text{scCO}_2$  is a very nonpolar fluid. Work by Yonker et al.<sup>8</sup> studied  $\text{scCO}_2$ ,  $\text{N}_2\text{O}$ ,  $\text{CCl}_3\text{F}$ , and  $\text{NH}_3$  and later<sup>9</sup> Xe,  $\text{SF}_6$  and ethane. Both studies observed the same relationship between density and polarizability for these fluids although  $\text{SF}_6$  and Xe were found to be less polar than  $\text{CO}_2$ . The polarizability results were fitted to a McRae–Bayliss model,<sup>10</sup> which showed two distinct regions where the clustering of solvent molecules around the indicator solute differed. This clustering of solvent molecules has been modeled by using a Langmuir isotherm.<sup>11</sup> The solvatochromic behavior of binary supercritical fluids has also been measured by a number of groups.<sup>12–14</sup>

Eckert and co-workers in 1983 discovered large negative partial molar volumes for naphthalene in sc ethylene caused by solvent clustering around the solute.<sup>15</sup> Since then many techniques, such as infrared<sup>12,16,17</sup> and fluorescence spectroscopy,<sup>18–21</sup> have been used to study intermolecular interactions in sc fluids. This work has shown that around the critical density there is a marked local density augmentation about the solute such that the local solvent density is considerably higher than the bulk value.<sup>22–24</sup> Recently such methods as integral equations and

fluctuation analysis have been used to model the solute–fluid interactions.<sup>25–27</sup> Statistical thermodynamics has proven to be a powerful tool when examining both the structure and dynamics of the solute–solvent environment in supercritical fluids. For a comprehensive theoretical treatise on the effect of supercritical solvent density inhomogeneities on solute dynamics, a recent review is recommended.<sup>28</sup>

The problem encountered with several of the sc fluids commonly used is that the low polarity precludes the dissolution of many polar solutes. In general, the more polar the fluid, the higher the critical temperature. Studies are currently being carried out with halogenated aliphatic compounds, which are slightly more polar but still have readily accessible critical constants. The solvent properties have so far only been measured for a limited number of fluids<sup>8,11</sup> such as  $\text{CF}_3\text{H}$  ( $\epsilon_c = 3.5$ ,  $T_c = 25.6$  °C,  $P_c = 47.8$  bar) and  $\text{CCl}_3\text{F}$  ( $T_c = 28.9$  °C,  $P_c = 37.7$  bar).

In the current work we report the solvent properties of 1,1,1,2-tetrafluoroethane (HFC 134a), which is extensively used as a refrigerant replacement as it is environmentally benign. This solvent has a relatively low critical temperature and pressure ( $T_c = 101.0$  °C,  $P_c = 40.55$  bar) yet is more polar ( $\epsilon_c = 5.0$ ) than the chlorofluorocarbons (CFCs) previously studied. The relative permittivity and  $\pi^*$  of HFC 134a are related by using the Kirkwood function and a hard sphere approximation model. The data obtained are also correlated to the solubility of water in sc HFC 134a.

## Experimental Section

A Beckman Model DU 650 spectrophotometer was used to measure the solvatochromic shift in the visible absorbance spectrum. Light was fed in to and out of the high-pressure cell by fiber optic cables (Hellma, Müllheim, FRG) fitted with a 662 QX prism adapter. The high-pressure cell was constructed from brass and 316 stainless steel with 1 cm thick sapphire windows and copper gas seals. The cell path length was 1 cm and the cell volume was approximately 1  $\text{cm}^3$ . Pressure was applied with a model 10–600 pump (Hydraulic Engineering Corp., Los Angeles), driven by compressed air. The temperature of the cell was measured using an Fe/constantan thermocouple and retained at a given temperature ( $\pm 0.5$  °C) by using a CAL 9900 heater. The pressure was monitored ( $\pm 2$  bar) by using a

\* Corresponding author: Fax +44 116 252 3789; E.mail apa1@le.ac.uk.

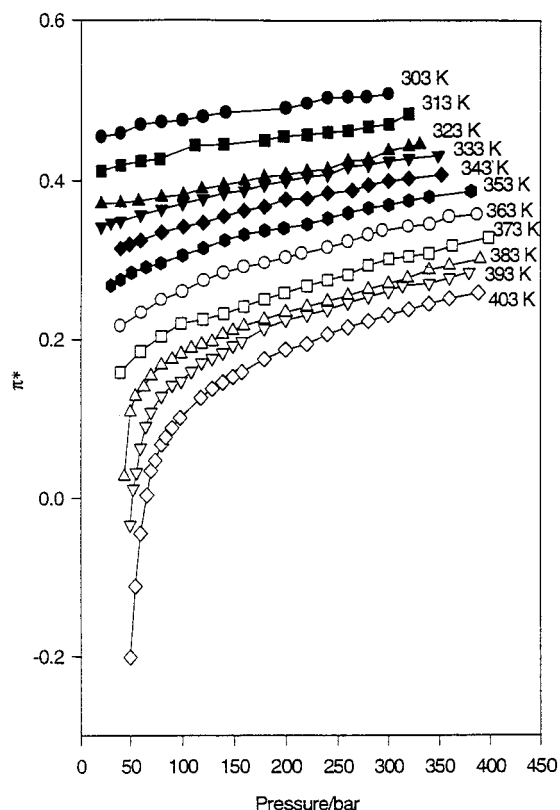


**Figure 1.** Effect of pressure on  $\pi^*$  for HFC 134a at various temperatures.

UCC-type PGE 1001.600 gauge. The solvent, HFC 134a (ICI Klea group, 99.99%), and the indicator, Nile Red (Aldrich), were used as received. Values of the relative permittivity of the solvent were measured by using a cell similar to one described previously.<sup>29</sup> Cell capacitances were measured at 65 kHz using a 1254 frequency response analyzer and a 1286 potentiostat (both Solartron Instruments). The electrodes were made of nickel, each with an area of 7.5 cm<sup>2</sup>, and there was a 1 mm gap between the electrodes. Values of solution density were taken from the literature.<sup>30</sup>

## Results and Discussion

The values of  $\pi^*$  were calculated from

$$\pi^* = \frac{\nu_{\max} - \nu_0}{s} \quad (1)$$

where  $\nu_{\max}$  and  $\nu_0$  are the wavenumbers of the absorbance maxima in the test solvent and reference solvent (cyclohexane), respectively and  $s$  is the susceptibility constant obtained from experiment. Nile Red<sup>31</sup> ( $s = -2300 \text{ cm}^{-1}$  and  $\nu_0 = 20.51 \times 10^3 \text{ cm}^{-1}$ ) was chosen as an indicator solute as it has previously been shown to be suitable for studies of sc fluids and gives a higher resolution than most other solutes. Figure 1 shows the values of  $\pi$  for HFC 134a as a function of temperature and pressure. At ambient temperatures and moderate pressure (10 bar) the  $\pi^*$  value is 0.45, which is comparable with the values for solvents such as ethyl acetate, butylamine and *p*-xylene.<sup>5</sup> As expected, the  $\pi^*$  value in the liquid region increases roughly linearly with increasing pressure in the liquid state. The value of  $\pi^*$  decreases dramatically at temperatures above 100 °C and below 60 bar. HFC 134a shows a large change in solvent properties over a relatively small temperature and pressure range, suggesting that it would be a useful solvent for extraction purposes.

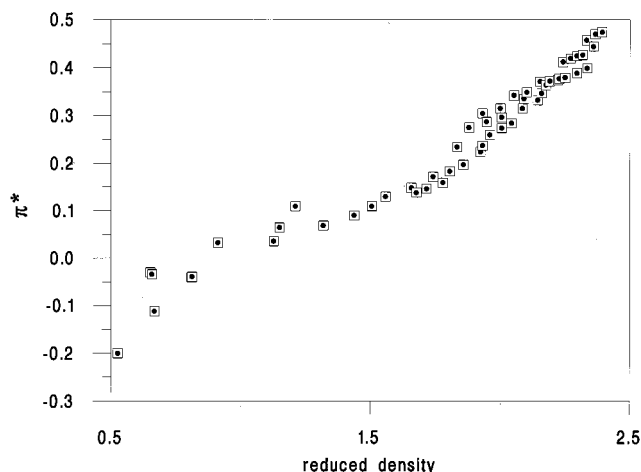


**Figure 2.** Effect of reduced density on  $\pi^*$  for HFC 134a.

Other groups that have studied the effect of temperature and pressure on the solvent properties of supercritical fluids have found that there are two or three density regions with markedly different solvent properties. Figure 2 shows the dependence of  $\pi^*$  on reduced density ( $\rho_r = \rho/\rho_c$ ; for HFC 134a  $\rho_c = 515.25 \text{ kg m}^{-3}$ ) for HFC 134a over the range 30–130 °C and 40–300 bar. Three distinct density regions can be observed with boundaries at reduced densities of approximately 1 and 2, yielding a shape indicative of local density augmentation.<sup>24</sup> The liquidlike region ( $\rho_r > 2$ ) has a steep slope. For dilute supercritical fluid solutions in this region, the bulk fluid density and local solvent density about the indicator solute have been shown to be very similar. The slope is less steep in the near-critical region ( $1 < \rho_r < 2$ ), where the local solvent density about the solute is believed to be considerably higher than the bulk value due to clustering. This is caused by attractive interactions between Nile Red and HFC 134a. The free volume and compressibility are much larger in this region. Hence the molecules can move into more energetically favorable positions with less resistance than in an incompressible liquid. In the gaslike region ( $\rho_r < 1$ ) the slope again increases, inferring that the local density is approaching that of the bulk as  $\rho_r$  tends to zero.

These regions are less clearly defined than those observed for  $\pi^*$  and other solvent parameters in CO<sub>2</sub>, Xe, and ethane.<sup>9,19</sup> This is probably because HFC 134a is a more polar molecule and the solvent–solvent interactions are larger than in less polar solvents. In NH<sub>3</sub> no discontinuous changes in  $\pi^*$  were observed with reduced density,<sup>9</sup> suggesting that the solvent–solute interactions are similar in magnitude to the solvent–solvent interactions.

Figure 3 shows the bulk relative permittivity of HFC 134a as a function of pressure at various temperatures. The forms of these isotherms are similar to those observed in Figure 1, but Figure 4 shows that these two parameters are not directly proportional to each other. Figure 5 shows that there are no distinct changes in relative permittivity with reduced density as observed with  $\pi^*$ . This is expected since relative permittivity is a bulk property of the solvent, whereas  $\pi^*$  is determined by local solute–solvent interactions. The data from Figure 5 were found to fit well to a polynomial expression similar to the Clausius–Mossotti equation, of the form

$$(\epsilon - 1)/(\epsilon + 2) = A + B\rho + C\rho^2 + \dots \quad (2)$$

and the constants were found to be  $A = 0.496$ ,  $B = -1.66 \times 10^{-4} \text{ kg}^{-1} \text{ m}^3$ , and  $C = 3.0 \times 10^{-7} \text{ kg}^{-2} \text{ m}^3$ .<sup>6</sup> This was found

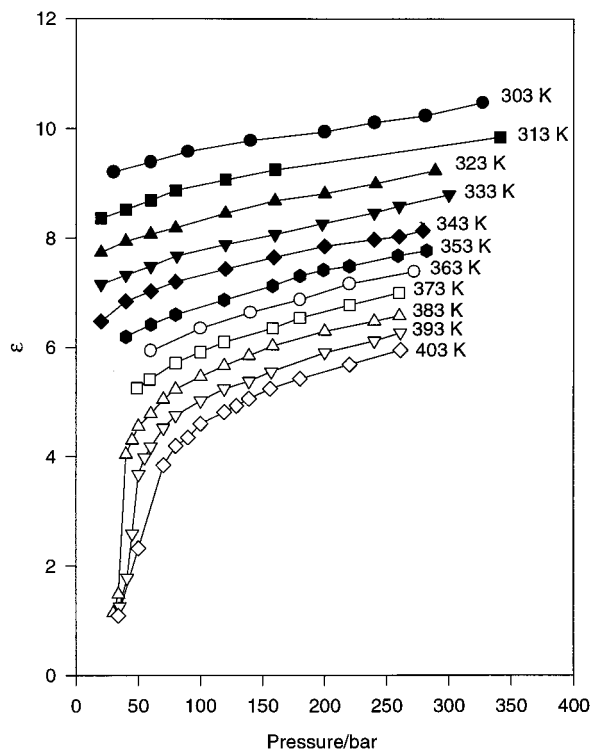


**Figure 3.** Bulk relative permittivity of HFC 134a as a function of temperature and pressure (symbols are the same as in Figure 1).

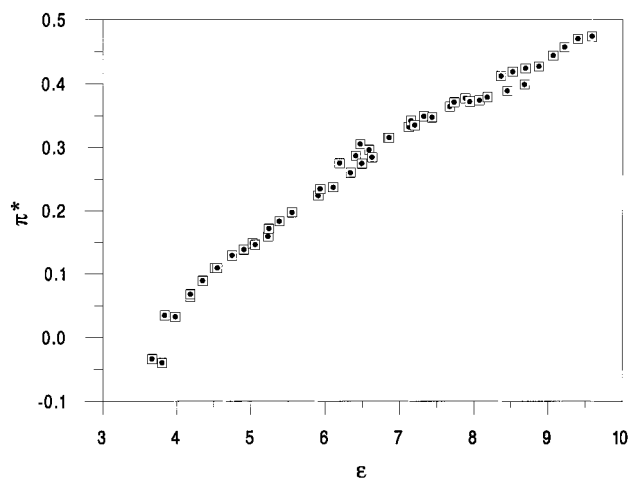


**Figure 4.**  $\pi^*$  as a function of bulk relative permittivity of HFC 134a.

to be applicable to all the data in the range 30–130 °C and 40–300 bar.

Yonker and Smith analyzed  $\pi^*$  values for CO<sub>2</sub>, SF<sub>6</sub>, and ethane using the McRae–Bayliss description of solvatochromism.<sup>10</sup> It was shown that  $\pi^*$  could be related to the refractive index,  $n$ , of the solvent by

$$\pi^* = \pi^*_{\text{gas}} + \frac{1}{2s} \left( AL_0 + \frac{\mu_G - \mu_E^2}{hca^3} \right) F_0 \quad (3)$$

where  $F_0 = 2(n^2 - 1)/(2n^2 + 1)$ ,  $\pi^*_{\text{gas}}$  is the vapor phase limit,  $L_0$  is a weighted mean wavelength,  $\mu_G$  and  $\mu_E$  are the dipole moments of the solute in the ground and excited states,  $c$  is the speed of light in a vacuum,  $a$  is the radius of the cavity occupied by the solute,  $h$  is Planck's constant, and  $A$  is the polarizability effect constant. A plot of  $\pi^*$  versus  $F_0$  showed that two regions

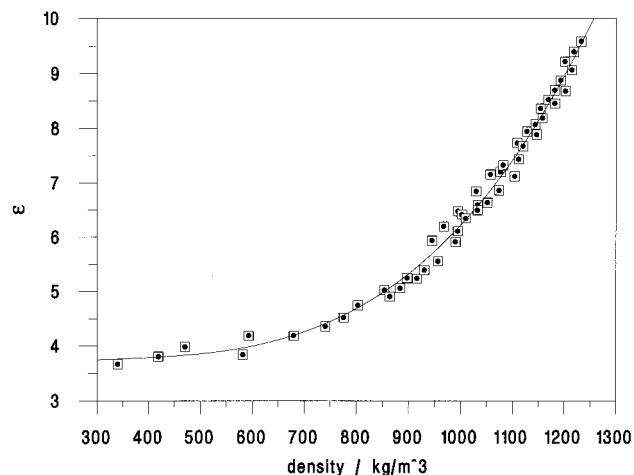


**Figure 5.** Bulk relative permittivity of HFC 134a as a function of density.

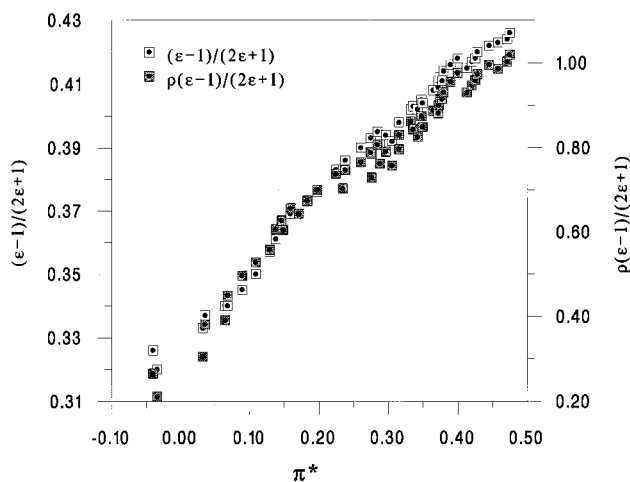


**Figure 6.** Plot of  $(\epsilon - 1)/(2\epsilon + 1)$  (white squares with black dots) and  $(\epsilon - 1)/(2\epsilon + 1)\rho_r$  (shaded squares with black dots) versus  $\pi^*$  for HFC 134a for the data shown in Figure 1.

of solvation were present in the supercritical state. The slopes of these plots were also shown to be at variance with those measured in the liquid state. The break in slope was proposed to originate from cluster formation of the solvent around the solute and hence a transition from gaslike to liquidlike behavior.

It has been shown<sup>32</sup> that the reaction field,  $R$ , created by an electrostatic field of polar molecules surrounding a solute is given by

$$R = \frac{2(\epsilon - 1)\mu_G}{(2\epsilon + 1)a^3} \quad (4)$$

If the reaction field is responsible for the stabilization of the excited state of the indicator solute, then  $\pi^*$  should be correlated to the Kirkwood function,  $((\epsilon - 1)/(2\epsilon + 1))$ . Figure 6 shows that there is a good correlation between these two parameters for fluids with  $\rho_r > 1.3$ . This includes data from both the liquid and supercritical states. The breakdown of this simple model at low reduced densities is probably caused by local solvent density augmentation.  $\pi^*$  is only strongly correlated to the Kirkwood function at high  $\rho_r$ , where both the local and bulk solvent density are roughly equal. Another cause of the failure of this model at low  $\rho_r$  could be an increase in the average solvent–solute separation distance; i.e., the cavity size increases. If the

latter case is accurate then the radius of the cavity will be given by

$$a^3 = M/N_A \rho \quad (5)$$

where  $M$  is the molar mass and  $N_A$  is the Avogadro constant. Hence  $\pi^*$  will be proportional to the Kirkwood parameter multiplied by the reduced density. Figure 6 shows that the linear correlation between  $\pi^*$  and this modified parameter ( $r = 0.984$ ) is worse than that for  $\pi^*$  and the simple Kirkwood parameter ( $r = 0.993$ ). This suggests that these deviations are due to solvent clustering and not expansion of the solvation cavity.

A more complex model is thus required to simulate the behavior of fluids close to the critical point. The properties of sc fluids have also been correlated to Dimroth's  $E_T$  and  $E'_T$  polarity scales,<sup>33</sup> and this has given similar results to the  $\pi^*$  findings. This is not surprising, as both scales are based upon the same principle and a strong correlation between the two has previously been demonstrated.<sup>17,34</sup> Recent work by Streck and Richert<sup>33</sup> has shown that  $E_T$  thermochromic shifts in liquid 2-methyltetrahydrofuran can be modeled by using a mean sphere approximation (MSA). This is a model developed by Wertheim<sup>35</sup> and used in many different forms to model solvent properties. In the form used by Streck and Richert, the Gibbs energy of solvation is characterized using the hard sphere radius of the solvent,  $d$ , and the relative permittivity of the solvent,  $\epsilon$ . It can be shown that the absorption maximum of the solute in the solvent can be related to a complex function of the solution relative permittivity,  $\alpha(\epsilon)$ , by

$$v_{\max} = v_{\text{gas}} + \frac{2\alpha(\epsilon)\mu_G(\mu_G - \mu_E)}{4\pi\epsilon_0 chD^3} \quad (6)$$

where  $v_{\text{gas}}$  is the absorption maximum of the solute in a vacuum,  $D$  is the radius of the solute, and  $\epsilon_0$  is the permittivity of free space. The function  $\alpha(\epsilon)$  is given by

$$\alpha(\epsilon) = \frac{8(\epsilon - 1)}{2uR^3\rho^3 + 2\epsilon[1 + R(1 - 2u)]^3 + [1 + R\rho]^3} \quad (7)$$

where  $R = d/D$ ,  $\rho = (1 - u)/(1 - 2u)$ ,  $u = 3\xi/(1 + 4\xi)$ ,  $\xi = 1/2[1 - 9/(4 + f^{1/3} + f^{-1/3})]$ , and  $f = 1 + 54\epsilon^{1/2}[1 - (1 + (1/27\epsilon^{1/2}))^{1/2}]$ . The value of  $R$ , the ratio of the radii of HFC 134a and Nile Red, was calculated to be 0.601.<sup>36</sup> Hence, for a given solute in a specific solvent  $\pi^*$  should be proportional to  $\alpha(\epsilon)$ . By combination of eqs 6 and 1 it can be seen that

$$\pi^* = \pi^*_{\text{gas}} + \frac{2\alpha(\epsilon)\mu_G(\mu_G - \mu_E)}{s4\pi\epsilon_0 chD^3} \quad (8)$$

Figure 7 shows the linear correlation between  $\pi^*$  and  $\alpha(\epsilon)$  via eq 8 for Nile Red in HFC 134a over the range 30–130 °C and 40–300 bar. It can clearly be seen that there is an excellent correlation ( $r = 0.997$ ), showing that the change in solvent properties between the liquid and supercritical states can be almost totally accounted for by the corresponding change in relative permittivity and density. This is a surprising result considering the very large range in density over which this model appears to be valid (275–1300 kg m<sup>-3</sup>). The value of  $\pi^*_{\text{gas}}$  was found to be  $-0.80$ , which is very similar to values reported by other studies<sup>10</sup> and close to the theoretical value of  $-1.06$ .<sup>8,37</sup>

It is by no means envisaged that the model proposed here is valid for all supercritical fluids under all conditions, but for

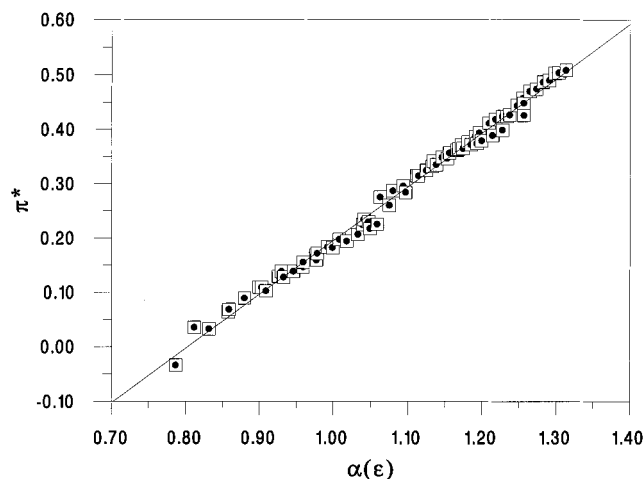


Figure 7. Plot of  $\alpha(\epsilon)$  vs  $\pi^*$  for HFC 134a for the data shown in Figure 1.

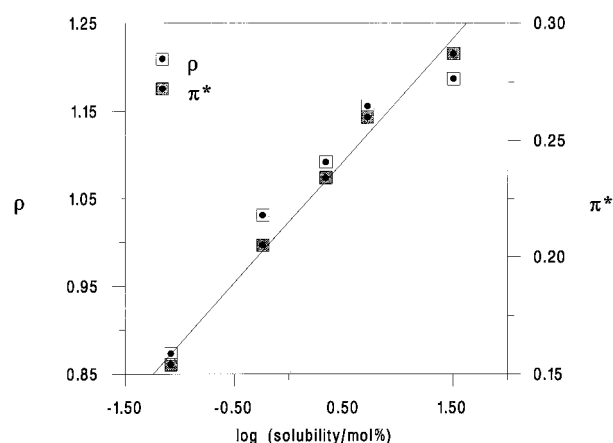


Figure 8. Correlation between the solubility of water at 383 K in HFC 134a with  $\pi^*$  and solvent density (in grams per cubic centimeter).

relatively large solvent molecules with negligible hydrogen-bond donor or acceptor characteristics with small solutes the model is clearly a very accurate method of predicting solvent polarity.

For this work to be useful,  $\pi^*$  must be an accurate guide to solvent properties. Jackson et al. recently studied the solubility of water in HFC 134a and found a correlation between log solubility and density, although deviations occurred at high density.<sup>38</sup> Figure 8 shows the linear correlation between log solubility and  $\pi^*$  for the same data at 383 K. An improved correlation is observed between  $\pi^*$  and log solubility ( $r = 0.994$ ) over density and log solubility ( $r = 0.968$ ) as reported by Jackson et al. This demonstrates that relative permittivity data can be used to accurately predict  $\pi^*$  values and hence solubility.

## Conclusion

This work has shown that the solvent properties of HFC 134a can be modeled across a wide range of densities throughout the liquid and supercritical regions by assuming the solvent molecules are simple dipoles. Deviations occur from simple models at low reduced densities due to an incomplete solvation sheath. These deviations can be accounted for by using a mean sphere approximation. Values of  $\pi^*$  have been shown to correlate well with solubility data for water in HFC 134a.

**Acknowledgment.** We thank the EPSRC for funding this work (via Grant GR/K05580) and a studentship (C.A.E.) and



ICI Klea for supplying the HFC 134a. The assistance of Mr. Richard Tooth in making some of the relative permittivity measurements is gratefully acknowledged.

## References and Notes

- (1) Taylor, L. T. *Supercritical Fluid Extraction*; John Wiley & Sons: New York, 1996.
- (2) McHugh, M. A.; Krukonis, V. J. *Supercritical Fluid Extraction*; Butterworth Heinemann: Boston, MA, 1994.
- (3) Yonker, C. R.; Wright, B. W.; Udseth, H. R.; Smith, R. D. *Ber. Bunsen-Ges. Phys. Chem.* **1984**, 88, 908.
- (4) Wright, B. W.; Smith, R. D. *Chromatographia* **1984**, 18, 542.
- (5) Kamlet, M. J.; Abboud, J.-L. M.; Taft, R. W. *J. Am. Chem. Soc.* **1977**, 99, 6027.
- (6) Laurence, C.; Nicolet, P.; Dalati, M. T.; Abboud, J.-L. M.; Notario, R. *J. Phys. Chem.* **1994**, 98, 5807.
- (7) Sigman, M. E.; Lindley, S. M.; Leffler, J. E. *J. Am. Chem. Soc.* **1985**, 107, 1471.
- (8) Yonker, C. R.; Frye, S. L.; Kalkwarf, D. R.; Smith, R. D. *J. Phys. Chem.* **1986**, 90, 3022.
- (9) Smith, R. D.; Frye, S. L.; Yonker, C. R.; Gale, R. W. *J. Phys. Chem.* **1987**, 91, 3059.
- (10) Yonker, C. R.; Smith, R. D. *J. Phys. Chem.* **1988**, 92, 235.
- (11) Kajimoto, O.; Futakami, M.; Kobayashi, T.; Yamasaki, K. *J. Phys. Chem.* **1988**, 92, 1347.
- (12) Blitz, J. P.; Yonker, C. R.; Smith, R. D. *J. Phys. Chem.* **1989**, 93, 6661.
- (13) Yonker, C. R.; Smith, R. D. *J. Phys. Chem.* **1988**, 92, 2374.
- (14) Ikushima, Y.; Saito, N.; Arai, M. *Bull. Chem. Soc. Jpn.* **1993**, 66, 1817.
- (15) Eckert, C. A.; Ziger, D. H.; Johnston, K. P.; Ellison, T. K. *Fluid Phase Equilib.* **1983**, 14, 167.
- (16) Ikushima, Y.; Saito, M.; Arai, N.; Arai, M. *Bull. Chem. Soc. Jpn.* **1991**, 64, 2224.
- (17) Ikushima, Y.; Saito, N.; Arai, M. *J. Phys. Chem.* **1992**, 96, 2293.
- (18) Zagrobelny, J.; Betts, T. A.; Bright, F. V. *J. Am. Chem. Soc.* **1992**, 114, 5249.
- (19) Sun, Y.; Bunker, C. E.; Hamilton, N. B. *Chem. Phys. Lett.* **1993**, 210, 111.
- (20) Heitz, M. P.; Bright, F. V. *J. Phys. Chem.* **1996**, 100, 6889.
- (21) Brennecke, J. F.; Eckert, C. A. *Proceedings of the International Symposium on Supercritical Fluids (I)*, Nice, France; Perrut, F., Ed.; Soc. Franc. Chim. 1988; p 263.
- (22) Knutson, B. L.; Tomasko, D. L.; Eckert, C. A.; Debenedetti, P. G.; Chialvo, A. A. *ACS Symp. Ser.* **1992**, 488, 60.
- (23) Kim, S.; Johnston, K. P. *AIChE J.* **1987**, 33, 1603.
- (24) Bennet, G. E.; Johnston, K. P. *J. Phys. Chem.* **1994**, 98, 441.
- (25) O'Brien, J. A.; Randolph, T. W.; Carlier, C.; Ganapathy, S. *AIChE J.* **1993**, 39, 1061.
- (26) Chialvo, A. A.; Cummings, P. T. *AIChE J.* **1994**, 40, 1558.
- (27) Petsche, I. B.; Debenedetti, P. G. *J. Chem. Phys.* **1989**, 91, 7075.
- (28) Tucker, S. C.; Maddox, M. W. *J. Phys. Chem. B* **1998**, 102, 2437.
- (29) Abbott, A. P.; Harper, J. C. *J. Chem. Soc., Faraday Trans.* **1996**, 92, 3895.
- (30) Tillner-Roth, R.; Baehr, H. D. *J. Chem. Thermodyn.* **1993**, 25, 277.
- (31) Deye, J. F.; Berger, T.; Anderson, A. G. *Anal. Chem.* **1990**, 62, 615.
- (32) Smith, R. D.; Yonker, C. R. *J. Phys. Chem.* **1989**, 93, 1261.
- (33) Streck, C.; Richert, R. *Ber. Bunsen-Ges. Phys. Chem.* **1994**, 98, 619.
- (34) Abboud, J.-L. M.; Kamlet, M. J.; Taft, R. W. *J. Am. Chem. Soc.* **1977**, 99, 8325.
- (35) Wertheim, M. S. *J. Chem. Phys.* **1971**, 55, 4291.
- (36) Edwards, J. T. *J. Chem. Educ.* **1970**, 47, 261.
- (37) Essfar, M.; Guiheneuf, G.; Abboud, J.-L. M. *J. Am. Chem. Soc.* **1982**, 104, 6786.
- (38) Jackson, K.; Bowman, L. E.; Fulton, J. L. *Anal. Chem.* **1995**, 67, 2368.